Acta Crystallographica Section D
Biological Crystallography
ISSN 0907-4449

Structure of cyclophilin from *Leishmania donovani* bound to cyclosporin at 2.6 Å resolution: correlation between structure and thermodynamic data

Vandavasi Venugopal,[a] Alok K. Datta,[b] Dhananjay Bhattacharyya,[c] Dipak Dasgupta[c]* and Rahul Banerjee[a]*

[a]Crystallography and Molecular Biology Division, Saha Institute of Nuclear Physics, Sector 1, Block AF, Bidhannagar, Kolkata 700 064, India, [b]Indian Institute of Chemical Biology, 4 Raja S. C. Mullick Road, Kolkata 700 032, India, and [c]Biophysics Division, Saha Institute of Nuclear Physics, Sector 1, Block AF, Bidhannagar, Kolkata 700 064, India

Correspondence e-mail: dipak.dasgupta@saha.ac.in, rahul.banerjee@saha.ac.in

Received 19 June 2009
Accepted 26 August 2009

PDB Reference: cyclophilin–cyclosporin A complex, 3eov, r3eovsf.

Drug development against *Leishmania donovani*, the pathogen that causes visceral leishmaniasis in humans, is currently an active area of research given the widespread prevalence of the disease and the emergence of resistant strains. The immunosuppressive drug cyclosporin is known to have antiparasitic activity against a variety of pathogens. The receptor for cyclosporin is the protein cyclophilin, which is a ubiquitous peptidylprolyl isomerase. The crystal structure of cyclophilin from *L. donovani* complexed with cyclosporin has been solved at 2.6 Å resolution. The thermodynamic parameters of the interaction have been determined using spectroscopic and calorimetric techniques. A detailed effort has been made to predict the thermodynamic parameters of binding from computations based on the three-dimensional crystal structure. These results were in good agreement with the corresponding experimental values. Furthermore, the structural and biophysical results have been discussed in the context of leishmanial drug resistance and could also set the stage for the design of potent non-immunosuppressive antileishmanials.

1. Introduction

Leishmania spp. are pathogens that cause a wide spectrum of diseases referred to as leishmaniasis. The most virulent form of these is visceral leishmaniasis (VL) or kala-azar arising from *Leishmania donovani*, which can be lethal if not correctly diagnosed and treated in time. Another complication is the growing resistance (Sundar & Murray, 2005) of the pathogen to traditional drug regimes and its synergism with HIV. Given the phenomenon of pathogenic resistance, the epidemiological status of the disease and the availability of only a few second-line drugs, it is imperative to continue the search for cheaper and more effective drug regimes with minimal side effects.

Cyclosporin A (CsA), a cyclic undecapeptide originally isolated from the fungus *Tolypocladium inflatum*, exhibits potent antiparasitic activity to varying degrees against a variety of protozoa and helminths (Page *et al.*, 1995), in addition to being immunosuppressive in humans. The receptor for cyclosporin A is the ubiquitously found protein cyclophilin (CyP), which primarily functions as a peptidyl-prolyl *cis–trans* isomerase (PPIase). CyPs are highly conserved phylogenetically and have been implicated in a plethora of cellular functions such as cell signalling, chaperone activity *etc.* (Wang & Heitman, 2005). Recent studies have shown the involvement of CyPs in the regulation and maintenance of mitochondrial transition pores (Du *et al.*, 2008). In addition, human cyclophilins have been demonstrated to be functionally associated with HIV-1 virions and to regulate HIV-1 infectivity (Keckesova *et al.*, 2006). The native enzymatic function of CyPs is inhibited by CsA as there is considerable overlap

between the active site of the protein and the CsA-binding pocket. However, the precise mechanism by which CsA exerts its antiparasitic activity and its variable efficacy against different organisms remains in need of further elucidation.

Several crystal and NMR structures of CyPs from a variety of sources have been solved (Ke, 1992; Kallen *et al.*, 1998). Similar to other CyPs, cyclophilin from *L. donovani* (LdCyP) is composed of an eight-stranded β-barrel with two α-helices located at either end of the barrel (Venugopal *et al.*, 2007). The native active site of the enzyme and the binding site for CsA lie on the face of the barrel, with the core of the barrel being inaccessible to solvent. Both the hydrophobic interior located inside the barrel and the CsA-binding site show a high degree of sequential and structural conservation across species, with variability primarily being present in the loop regions.

CsA binds to human CyP with high affinity (Wear & Walkinshaw, 2006) and similar experiments indicate comparable binding affinities to the parasitic enzyme LdCyP. CsA cannot be used as an antileishmanial directly, owing to its immunosuppressive activity in humans, which results from the binding and inhibition of human calcineurin by the CyP–CsA binary complex, curtailing further downstream processes. There is relatively little information available regarding the status of calcineurin (Cn) in *Leishmania*. Recently, the genomes of several protozoa have been sequenced (*L. major*, *L. infantum*, *L. braziliensis*, *Trypanosoma cruzi etc*.) and are currently available in the public domain (GeneDB). Analysis of these genomes indicates the presence of calcineurin homologues with about 50% sequence identity with respect to human calcineurin.

Considerable effort has gone into the design of CsA derivatives that exhibit reduced immunosuppressive activity in humans, in all probability owing to the low affinity of the CyP–(CsA derivative) complex for calcineurin. Interestingly, CsA derivatives obtained by minor chemical modifications to CsA can discriminate between mammalian and parasitic calcineurin. For example, the addition of a hydroxyl group to Mle4 (in CsA) enables binding to calcineurin in *Cryptococcus neoformans* with higher affinity and at the same time prevents interaction with the homologous mammalian protein (Cruz *et al.*, 2000). Several of these derivatives have been screened against protozoan parasites in order to evaluate their efficacy as potential therapeutic agents (Bua *et al.*, 2004, 2008).

Given the importance of the interaction of CsA with CyP, the present study characterizes in detail the molecular and structural basis of the CyP–CsA interaction in *L. donovani* both in biophysical and structural terms, with special emphasis on the prediction of thermodynamic parameters (enthalpy, heat capacity and free energy) of binding based on the crystal structure of the LdCyP–CsA complex at 2.6 Å resolution.

2. Materials and methods

2.1. Expression and purification

Recombinant cyclophilin from *L. donovani* cloned in vector pQE32 was overexpressed in *Escherichia coli* M15 cells as a His_6-tagged protein. The protein was purified to homogeneity using a nickel–nitrilotriacetic acid agarose column as per the manufacturer's suggested procedure. The purified LdCyP was then extensively dialyzed against buffer containing 20 m*M* Tris pH 8.5 and 0.02% NaN_3 for crystallization experiments. Alternatively, the protein was buffered in 25 m*M* potassium phosphate pH 7.5 for spectroscopic and calorimetric work.

Table 1
Summary of diffraction data and crystallographic refinement statistics.

PDB code	3eov
Space group	*C*121
Unit-cell parameters (Å, °)	a = 69.810, b = 83.125, c = 73.580, $\alpha = \gamma = 90$, $\beta = 103.03$
Resolution (Å)	30.00–2.60 (2.69–2.60)
No. of unique reflections	12040
Redundancy	4.11 (5.3)
$R_{\rm merge}$† (%)	5.2 (25.1)
Completeness (%)	95.3 (96.5)
$I/\sigma(I)$	14.1 (2.6)
σ cutoff (F)	2.00
No. of reflections (working)	11417
No. of reflections (test)	623
No. of protein atoms	2728
No. of water molecules	76
$R_{\rm cryst}/R_{\rm free}$‡ (%)	20.7/25.1
R.m.s. deviation from ideal values	
Bond lengths (Å)	0.008
Bond angles (°)	1.40
Dihedrals (°)	25.1
Impropers (°)	0.78
Mean B value (Å^2)	49.6
B from Wilson plot (Å^2)	52.4
Ramachandran plot§	
Most favoured (%)	77.4
Additional allowed (%)	21.2
Generously allowed (%)	1.5
Residues truncated to Ala	Glu22, Gln81

† $R_{\rm merge} = \sum_{hkl}\sum_i |I_i(hkl) - \langle I(hkl)\rangle| / \sum_{hkl}\sum_i I_i(hkl)$, where $I_i(hkl)$ and $\langle I(hkl)\rangle$ represent the diffraction-intensity values of the individual measurements and the corresponding mean values. The summation is over all unique measurements. ‡ $R_{\rm cryst} = \sum_{hkl} |F_{\rm obs} - F_{\rm calc}| / \sum_{hkl} |F_{\rm obs}|$; $R_{\rm free}$ is $R_{\rm cryst}$ for a 6% cross-validated test data set. § Ramachandran plot in *PROCHECK* (Laskowski *et al.*, 1993).

2.2. Crystallization and data collection of LdCyP–CsA

Cyclophilin, at about 15 mg ml^{-1} in the buffer mentioned above containing 5–7%(v/v) ethanol, was incubated with CsA in a 1:2 ratio for 30 min at room temperature. The solution was then centrifuged at 15 000g prior to setting up crystallization using the batch method at 293 K. The 50 µl total solution in each tube contained 10–12 mg ml^{-1} of the protein complexed with CsA, 100–150 m*M* NaCl, 10%(w/v) PEG 4000 and 5%(v/v) ethanol. Crystals appeared within 10 d and were mounted on glass capillaries (utilizing the same mother liquor as in the crystallization tubes) to collect diffraction data using a MAR image-plate scanner mounted on an in-house Rigaku Cu $K\alpha$ rotating-anode X-ray source. The distance between the crystal and detector was set to 200 mm, with an oscillation range of 1°. The data were processed using *AUTOMAR* in the Laue symmetry $C2/m$, with a final $R_{\rm merge}$ of 5.2% in the resolution range 30.0–2.60 Å. Data-collection statistics are summarized in Table 1.

2.3. Crystal structure solution and refinement

The crystal structure solution in space group *C*2 was obtained by molecular replacement (*AMoRe* from the *CCP*4 program suite) using native cyclophilin (LdCyP; PDB code 2haq; Venugopal *et al.*, 2007) as the search model. Two molecules were found in the asymmetric unit, giving a correlation coefficient and *R* factor of 67.4 and 37.5%, respectively. Attempts to place a third molecule in the asymmetric unit met with failure as no further change was recorded in the correlation coefficient and *R* factor. Prior to refinement, a 2σ cutoff was applied to remove 62 weak reflections that could possibly be liable to error. A total of 623 reflections (5.2%) were randomly flagged from the entire resolution range (30.0–2.60 Å) to calculate $R_{\rm free}$ (Brünger, 1992). A few cycles of rigid-body refinement were carried out in *CNS* (Brünger *et al.*, 1998) prior to the calculation of an electron-density map ($2F_{\rm o} - F_{\rm c}$). The quality of the map showed unambiguous electron density for CsA and almost all of the protein side chains without any discontinuities. Manual model building was performed using the program *O* (Jones *et al.*, 1991). Several iterations of model building and refinement (*CNS*) improved the electron-density significantly, enabling CsA to be modelled into the electron density. *R* and $R_{\rm free}$ at this stage of refinement were 28.5% and 31.5%, respectively. Subsequently, water molecules were identified and individual *B* factors were refined. The refinement was terminated after a last round of fitting performed on an OMIT map. The final model, with an *R* and $R_{\rm free}$ of 20.7% and 25.1%, respectively, consisted of 2558 protein atoms, 170 atoms of CsA and 76 water molecules in the asymmetric unit. The coordinates were deposited in the Protein Data Bank (PDB code 3eov) after validation using *PROCHECK* (Laskowski *et al.*, 1993). There were no residues present in the disallowed region of the Ramachandran plot and the r.m.s. deviations in bond lengths and bond angles were 0.008 Å and 1.4°, respectively. The refinement and structure-validation statistics are summarized in Table 1.

2.4. Spectroscopic measurements

All fluorescence spectra were measured on a Perkin–Elmer LS 55 luminescence spectrophotometer at constant temperature using a quartz cell of 1 cm path length. The excitation wavelength was 295 nm for the selective excitation of the lone tryptophan residue in LdCyP. Emission spectra were recorded in the range 310–450 nm. Both the excitation and the emission bandwidths were set to 10 nm.

2.4.1. Quantitative analysis of binding. A fixed concentration (3–4 µ*M*) of LdCyP in 25 m*M* potassium phosphate buffer pH 7.5 was titrated with increasing concentrations of CsA at 298 K. Prior to experiments, 100 µ*M* CsA stock solution was prepared in the same buffer containing 20% alcohol. The final concentration of ethanol did not exceed 2% in the experiments. The results of fluorometric titrations were analyzed and the dissociation constant ($K_{\rm d}$) was determined using a nonlinear curve-fitting algorithm as reported elsewhere (Aich *et al.*, 1992; Chakrabarti *et al.*, 2001). The binding stoichiometry corresponds to the intersection of the two straight lines (fitted by least squares) in the plot of the normalized increase in fluorescence *versus* the ratio of input concentrations of the ligand and protein.

2.4.2. Fluorescence quenching. Quenching studies of LdCyP in unligated and ligated forms were performed using acrylamide, a tryptophan-specific neutral quencher, at 298 K. Analysis of the fluorescence quenching was performed using the classical Stern–Volmer equation, $F_{\rm o}/F = 1 + K_{\rm sv}[Q]$, where F and $F_{\rm o}$ are the fluorescence intensities in the presence and absence of acrylamide, respectively, $[Q]$ is the molar concentration of acrylamide and $K_{\rm sv}$ is the collisional quenching constant (M^{-1}).

2.5. Isothermal titration calorimetry

Isothermal titration calorimetric experiments were performed using a high-precision VP-ITC system (Microcal Inc., Northampton, Massachusetts, USA) in order to determine the stoichiometry, dissociation constant and thermodynamic parameters of the association between LdCyP and CsA. Samples of LdCyP purified from a single batch were extensively dialyzed against phosphate buffer pH 7.5 at 277 K. CsA stock solution was prepared in ethanol and dissolved in the dialysis buffer to give a final concentration of 6 µ*M* with 1%(*v*/*v*) ethanol. The same amount of ethanol was added to the LdCyP sample in order to minimize the heat of dilution. CsA was taken in the sample cell owing to its very low solubility and was titrated with LdCyP in the injection syringe. Appropriate control experiments were performed without CsA in the sample cell to estimate the heat of dilution. The binding enthalpy for the CsA solution was corrected by subtracting the heat of dilution obtained from control experiments. The resulting corrected binding isotherm was fitted by a nonlinear least-squares analysis to a single-class binding-site model using the software (*Origin*) provided by Microcal.

2.6. Structure-based theoretical evaluation of thermodynamic parameters

2.6.1. Calculation of solvent-accessible surface area. The solvent-accessible surface areas (SAAs) were computed in accordance with the algorithm of Lee & Richards (1971) with a solvent probe of radius 1.40 Å. The assigned radii of the non-H atoms were nitrogen, 1.75 Å; oxygen, 1.60 Å; sulfur, 2.0 Å; methyl carbon, 2.0 Å; carbonyl carbon, 1.85 Å; all other C atoms, 1.92 Å. The coordinates for the LdCyP–CsA complex were obtained from PDB entry 3eov.

2.6.2. Calculation of desolvation free energy. The desolvation free energy $\Delta G_{\rm d}$ (1) was estimated based on the free energy of transfer (of reactants and products) from an aqueous medium to a reference medium. Based on the simple atomic solvation parameter (ASP) model (Vajda *et al.*, 1994), the free energy of transfer was

$$\Delta G_{\rm d} = \Delta G_{\rm transfer} = \sum \sigma_i \Delta A_i, \qquad (1)$$

where ΔA_i denotes the change in solvent-accessible surface area of the ith atomic group and σ_i is the corresponding ASP (Eisenberg & McLachlan, 1986). The ASP values used for the

Table 2
Contacts between LdCyp active-site residues and CsA within 3.8 Å in the crystal structure.

LdCyp	CsA	Distance (Å)
Arg78 CZ	Mle10 O	3.4
Arg78 NH1	Mle10 O	3.3 (hydrogen bond)
Arg78 NH2	Mle10 O	2.8 (hydrogen bond)
Phe83 CE2	Mle10 O	3.7
Phe83 CZ	Mle9 C	3.6
Phe83 CZ	Mle9 O	3.3
Phe83 CZ	Mva11 CG2	3.7
Gln86 CD	Mva11 CG1	3.5
Gln86 OE1	Mva11 CG1	3.3
Gln86 NE2	Bmt1 O	3.3 (hydrogen bond)
Gly95 O	Aba2 CA	3.6
Gly95 O	Aba2 C	3.4
Gly95 O	Sar3 N	3.1
Gly95 O	Sar3 CN	2.8
Ala123 CA	Mva11 O	3.6
Ala123 CB	Mva11 CG1	3.8
Ala123 CB	Mva11 O	3.6
Asn124 N	Mva11 O	3.5 (hydrogen bond)
Asn124 C	Aba2 N	3.5
Asn124 O	Bmt1 CA	2.9
Asn124 O	Bmt1 CB	3.2
Asn124 O	Bmt1 CD1	3.4
Asn124 O	Bmt1 C	3.1
Asn124 O	Aba2 N	2.6 (hydrogen bond)
Asn124 O	Aba2 CA	3.7
Asn124 O	Aba2 CB	3.7
Ala125 CA	Bmt1 CE	3.7
Gln133 CB	Aba2 CG	3.7
Gln133 CD	Aba2 CG	3.1
Gln133 OE1	Aba2 CG	3.3
Gln133 NE2	Aba2 CG	2.9
Phe135 CD2	Mva11 CG1	3.5
Trp143 CE2	Mle9 O	3.7
Trp143 CD1	Mle9 O	3.7
Trp143 NE1	Mle9 O	2.8 (hydrogen bond)
Trp143 CZ2	Mle9 CB	3.5
Trp143 CZ2	Mle9 CD1	3.6
His148 CE1	Mva11 CN	3.6
His148 CE1	Mva11 O	3.6
His148 NE2	Mva11 CN	3.4

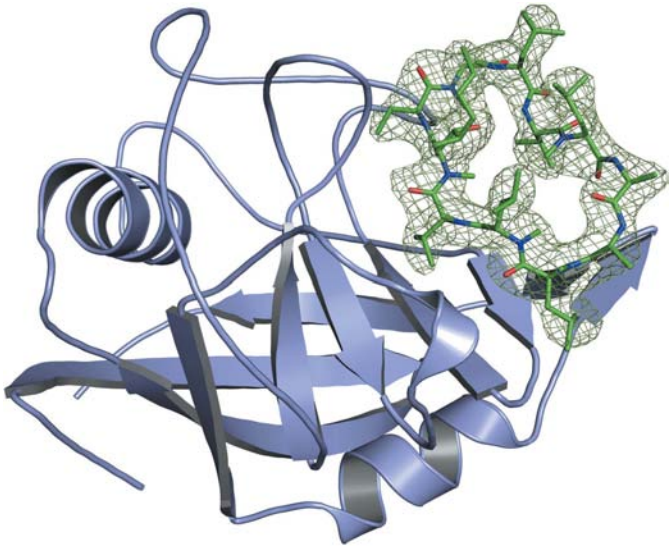

Figure 1
Crystal structure of the LdCyP–CsA complex at 2.6 Å resolution. CsA is shown in stick representation and the electron density around CsA (shown as a mesh) is contoured at the 2.0σ level from a $2F_o - F_c$ map. This figure was generated using *PyMOL* (DeLano, 2002).

various atomic groups were (in kcal mol^{-1} Å^{-2}; 1 cal = 4.186 J) $\sigma_C = 30.5 \pm 1.2$; $\sigma_{N/O} = -0.90 \pm 2.5$; $\sigma_{O^-} = -15.0 \pm 7.3$; $\sigma_{N^+} = -38.5 \pm 4.5$. In the case of $\Delta\tilde{G}_d$, σ_{O^-} and σ_{N^+} were not fed into expression (1) and all atoms were assigned the atomic solvation parameters of either $\sigma_C = 30.5 \pm 1.2$ or $\sigma_{N/O} = -0.90 \pm 2.5$ kcal mol^{-1} Å^{-2}. The transfer free energy then reduced to

$$\Delta\tilde{G}_d = (30.5 \pm 1.2)\Delta A_{nonpolar} - (0.9 + 2.5)\Delta A_{polar}, \quad (2)$$

where ~ indicates that the protonation/deprotonation effects of ionizable side chains have been neglected.

2.6.3. Calculation of electrostatic interaction energy. The electrostatic interaction energy $\Delta E_{el}^{r\text{-}l}$ was calculated using *CHARMM* v.30b1 (Brooks *et al.*, 1983) with the *CHARMM*-19 force field (polar H atoms). In the case of the unnatural amino acids in CsA {Mle: *N*-methylleucine; Mva: *N*-methylvaline; Sar: sarcosine; Aba: aminobutyric acid; Bmt: *N*-methyl-(4*R*)-4-[(*E*)-2-butenyl]-4,*N*-dimethyl-L-threonine; Dal: D-alanine} the partial charges for atoms corresponding to their closest natural counterparts (Ala for Aba; Ser for Bmt) were taken from *CHARMM*-19. The extra side-chain atoms were assigned Mulliken charges calculated by the B3LYP/6-31G(d,p) method (Hertwig & Koch, 1997) using the *GAUSSIAN*03 software, which were found to be in good agreement with the partial charges of similar atom types (apolar) from the *CHARM*-19 force field. The 'methylated amide group' was treated as a special case. The Mulliken charges were calculated for Ala-Ala-Ala and Ala-MeAla-Ala fragments. The Mulliken charges were observed to be −0.54 and −0.44 for the N atom in the protonated and methylated states, respectively. Hence, a value of +0.1 was added to the partial charge of the amide N atom (−0.35 as found in *CHARMM*-19) to obtain a value of −0.25 for use in calculations involving the methylated amide. The attached methyl group was assigned a value of +0.15 to maintain overall neutrality of the amino acid. The interaction energy was calculated with a distance-dependent dielectric coefficient $\varepsilon = 4r$ and a nonbonded distance cutoff of 17 Å. Prior to the calculation, the crystal structure of the complex (LdCyP–CsA) was energy-minimized to convergence by 100 steps of steepest-descent minimization followed by 10 000 steps of conjugate-gradient minimization.

2.6.4. Calculation of side-chain entropy. The conformational side-chain entropy for the protein amino-acid residues were calculated from the Pickett & Sternberg (1993) absolute scale of side-chain entropies, in which side-chain rotamer libraries are converted to entropies by the classical expression

$$S_c = -R \sum_i p_i \ln(p_i), \quad (3)$$

where p_i denotes the probability of the ith rotamer and R is the universal gas constant. Following the convention of Weng *et al.* (1997), the side-chain entropy S_c (from the Pickett & Sternberg scale) was considered to be ΔS_c if the change (ΔA_t) in the total solvent-accessible surface area of the side chain is more than 60% of the standard side-chain surface area A_t^*. The standard side-chain surface area A_t^* for every amino acid was calculated as the solvent-accessible area of the side chain in a fully extended conformation located in a Gly-Xaa-Gly

peptide fragment. In the case that ΔA_t was less than 60% of the standard side-chain surface area A_t^* then the entropy loss was scaled according to $\Delta S_c = \alpha S_c$, where $\alpha = \Delta A_t/(0.6A_t^*)$.

3. Results

3.1. Crystal structure of the LdCyP–CsA complex

The crystal structure of the LdCyP–CsA complex contained two molecules in the asymmetric unit with an r.m.s. deviation of 0.2 Å between them. The relative position of CsA with respect to CyP and their contacts with the protein were identical in both polypeptide chains. With the exception of Phe135 (χ_2), the torsion angles of the residues constituting the binding pocket were also in agreement.

The r.m.s. deviation between ligated and unligated CyPs is 0.4 Å, thereby indicating negligible changes in the overall secondary and tertiary structure of the protein upon binding to the ligand. The residues constituting the binding pocket are Arg78, Phe83, Gln86, Gly95, Ala123, Asn124, Ala125, Gln133, Phe135, Trp143 and His148. Most of these residues are either located in the β-sheet constituting one face of the barrel (Arg78, Gln86 and Phe135), in β-turns interconnecting the individual strands (Phe83, Ala123 and Gln133) or in loops (Gly95, Asn124, Ala125 and His148). Trp143, accommodated on the single turn of a 3_{10}-helix, is essential for the CyP–CsA interaction (Fig. 1). *E. coli* CyP, which has phenylalanine at the position corresponding to Trp143 in LdCyP, has negligible affinity for CsA and is also resistant to the drug (Fejzo *et al.*, 1994). It is probable that the essential role of Trp143 arises as a consequence of its formation of a hydrogen bond (NE1) to the carbonyl O atom of Mle9 in CsA, in addition to extensive van der Waals contacts. A total of five hydrogen bonds were observed between CsA and LdCyP (Table 2) out of a total of 40 contacts within 3.8 Å. Of the 11 residues in CsA, only six (Bmt1, Aba2, Sar3, Mle9, Mle10 and Mva11) come into contact with the protein. All binding-site residues and interactions are completely conserved in human (PDB code 2rma) and *T. cruzi* (PDB code 1xq7) CyP–CsA complexes.

As previously reported, native LdCyP is surrounded by a hydration shell composed of 114 solvent water molecules. At 2.6 Å resolution and with a substantially modified crystallization solution in the case of the LdCyP–CsA complex (containing 5–7% ethanol), 76 water molecules were identified in the asymmetric unit, with approximately 40 waters in the hydration shell of each chain. Of these, 46 water molecules (23 per chain) were conserved with respect to the native protein.

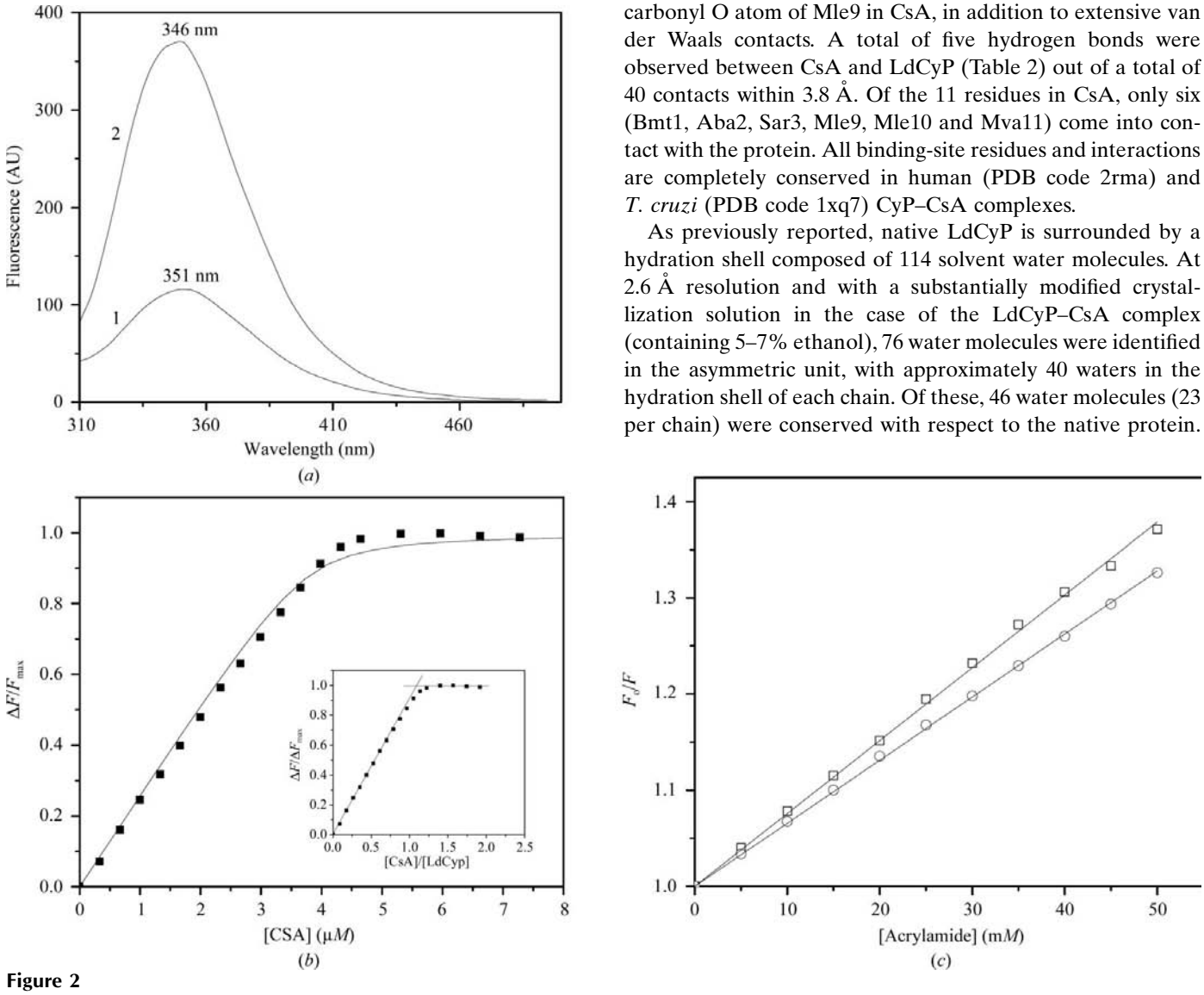

Figure 2
(*a*) Fluorescence enhancement of LdCyp upon complexation with CsA. Fluorescence spectra of native LdCyP (1) and LdCyP saturated with CsA (2). (*b*) Analysis of binding and stoichiometry for the association of LdCyp and CsA in 25 m*M* phosphate buffer pH 7.5. The normalized increase in the fluorescence of LdCyp is plotted against the molar concentration of CsA and the data points are fitted to a nonlinear curve. The inset panel illustrates the method of determining the binding stoichiometry. The abscissa value corresponding to the intersection of the two straight lines gives 1.12 for the binding stoichiometry. (*c*) Stern–Volmer plots for the acrylamide quenching of native LdCyp (squares) and LdCyp complexed with CsA (circles) at 298 K (λ_{ex} = 295 nm, λ_{em} = 340 nm).

All such conserved waters make two or more hydrogen bonds to protein atoms in both native and complexed LdCyP. Seven of these waters making four or more conserved hydrogen bonds form a stabilizing network by bridging loops L2–L3 (HOH 11, 20 and 34 in the native protein), L2–L4 (HOH 21 and 14), L1–L2 (HOH 3) and L3–L3 (HOH 7). This could be of structural significance as loops L2 (residues 88–118), L3 (123–133) and L4 (138–149) accommodate the active-site residues Gly95, Ala123, Asn124, Ala125, Gln133 and His148. HOH 11 (native protein) and the corresponding conserved waters (HOH 5 in chain *A* and HOH 22 in chain *B*) from the LdCyP–CsA complex make a maximum number of ten and six contacts with polar protein atoms, respectively. Two waters, HOH 7 and HOH 11, make direct contacts with the active-site residues Gln133 and Asn124, respectively. Two water molecules were found to be displaced from the active site of LdCyP upon complexation with CsA (HOH 70 and HOH 85 both make contacts with Asn124). However, at this resolution no waters that were in simultaneous contact with protein and drug could be found.

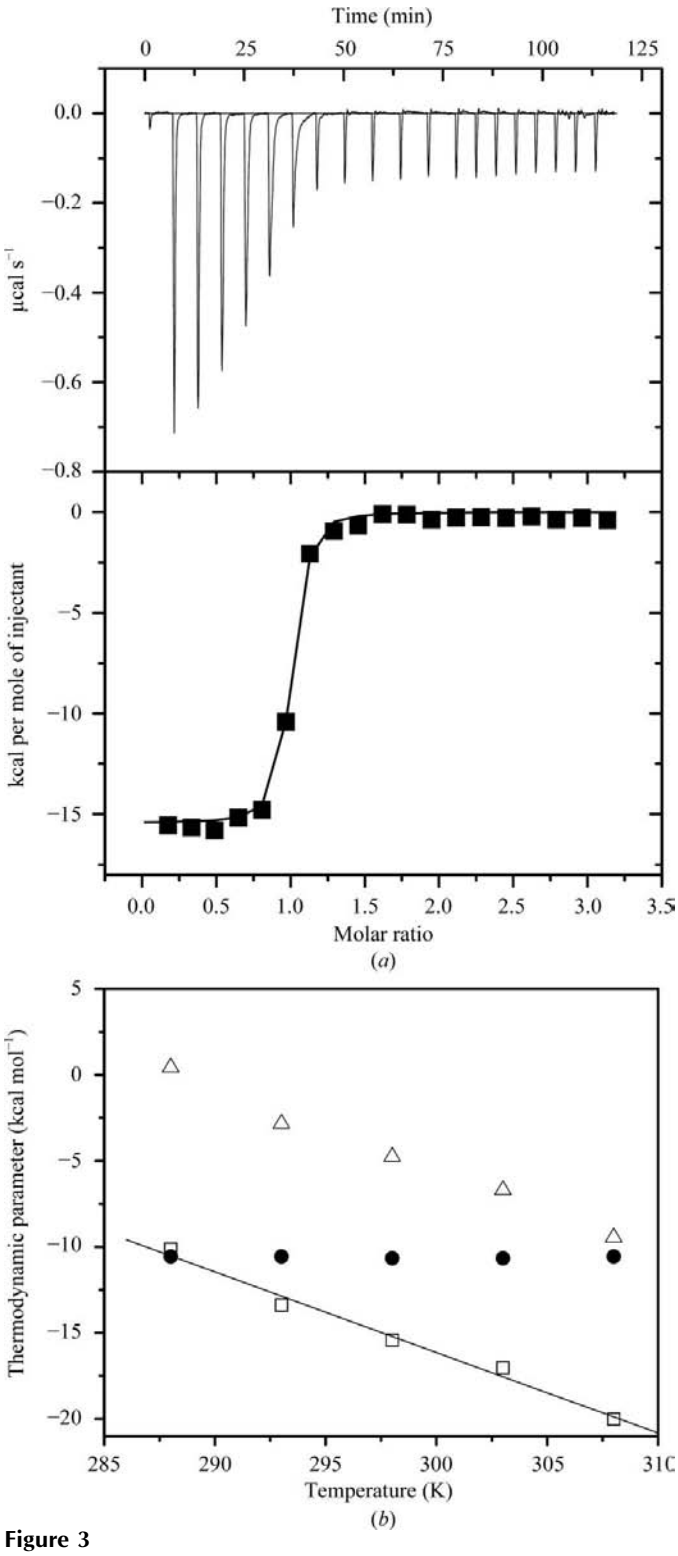

Figure 3
(*a*) Thermogram of the binding of LdCyP and CsA at 298 K in potassium phosphate buffer pH 7.5. The observed binding enthalpy was not corrected for the enthalpy of ionization as the buffer used (25 m*M* phosphate pH 7.5) has a very low ionization enthalpy ($\Delta H_{\rm ionization}$ = 1 kcal mol^{-1}). (*b*) Plot of $T\Delta S$ (triangles), ΔH (squares) and ΔG (filled circles) *versus* temperature. The slope of the plot ΔH *versus* T gives $\Delta C_{\rm p}$.

3.2. Fluorescence spectroscopic analysis of the association

The emission intensity of LdCyP increases upon addition of CsA as a result of formation of the complex. Concomitant with the increase in quantum yield, there is a blue shift of 5 nm of the emission peak (Fig. 2). The quenching constant for acrylamide accessibility to the single tryptophan (Trp143) residue also decreases from 7.4 to 6.4 M^{-1} upon complex formation. Increases in the quantum yield and the blue shift of the emission peak originate from alteration of the tertiary structure of the protein as a consequence of drug association. Similarly, the reduction in the Stern–Volmer constant indicates a reduction in the accessibility of the tryptophan residue to the neutral quencher. However, an insignificant change was observed in the tertiary structure of LdCyP upon drug binding, as seen in the crystal structure of the LdCyP–CsA complex. This apparent anomaly can be explained by the three-dimensional location of the lone fluorophore, Trp143, which lies exposed with a solvent-accessible area of 124.20 Å^2 in the binding pocket of free LdCyP. Upon binding to CsA, the solvent molecules around the fluorophore are displaced by CsA, increasing the hydrophobicity in the environment surrounding this residue, with a reduction in the solvent-accessible area to 79.20 Å^2. As a consequence, there is a decrease in the solvent accessibility of Trp143.

Fluorescence titration was employed to evaluate the dissociation constant ($K_{\rm d}$) for the LdCyP–CsA complex, which was found to be 63 n*M* (Fig. 2). Comparable values in the nanomolar range for the dissociation constant have been reported for the interaction between human CyP and CsA (Wear & Walkinshaw, 2006; Fanghanel & Fischer, 2003).

3.3. Thermodynamic parameters for LdCyP–CsA binding

The association of LdCyP and CsA has been characterized by ITC at different temperatures in order to determine the thermodynamic parameters of binding. Fig. 3(*a*) shows a representative titration curve that fits well to a 'single binding-site' model. The calculated stoichiometry of binding in all the

titrations had values between 0.94 and 1.1, in agreement with the value obtained from fluorescence titration. A titration at 298 K resulted in ΔH, $T\Delta S$ and ΔG of -15.4, -4.7 and -10.6 kcal mol^{-1}, respectively. The dissociation constant (K_d) value of 15.15 nM at 298 K also agrees fairly well with the value obtained from fluorescence titration. The results show that the LdCyP–CsA interaction is primarily enthalpy-driven. Fig. 3(*b*) shows plots of ΔH, $T\Delta S$ and ΔG against T. ΔG remains constant throughout the experimental range of temperatures, supporting enthalpy–entropy compensation for the system. There is a linear dependence of ΔH and ΔS on temperature. The slope for the plot of variation of ΔH with temperature gives the value of change in heat capacity, ΔC_p ($\Delta C_p = -468 \pm 30$ cal K^{-1} mol^{-1}) for the association. The large negative value of ΔC_p could be a consequence of the segregation of a considerable expanse of nonpolar surface area from solvent upon complexation owing to the predominance of hydrophobic interactions between the protein and drug. The thermodynamic parameters determined experimentally for the association of LdCyP and CsA are in good agreement with the values reported previously for CsA and human CyP (Wear & Walkinshaw, 2006; Fanghanel & Fischer, 2003).

3.4. Structure based prediction of thermodynamic parameters

3.4.1. Heat-capacity change ΔC_p. A significant body of literature exists correlating changes in heat capacity (ΔC_p) with the physical interactions involved in protein–ligand and protein–protein association based on high-resolution crystal structures. One of the most prominent observations refers to large changes in heat capacity arising from hydrophobic interactions. As is well known, hydrophobic interactions consist of two components: (i) desolvation of nonpolar protein atoms and (ii) their subsequent packing within proteins (or protein complexes) sequestered from the surrounding aqueous environment. Thus, the hydrophobic contribution to ΔC_p can effectively be estimated based on the burial of nonpolar solvent-accessible area upon folding or complexation. Several empirical formulations have been proposed calculated from the aqueous dissolution of model hydrophobic compounds. Solvent-accessible areas (SAAs) calculated for native (LdCyP) and complex (LdCyP–CsA) crystal structures show a total area (ΔSAA) of -1006 Å^2 (-432 Å^2 from LdCyP and -574 Å^2 from CsA) to be buried in the LdCyP–CsA interface upon complexation, of which $\Delta SAA_{nonpolar}$ and ΔSAA_{polar} are -681 and -325 Å^2, respectively. One formulation which includes both nonpolar and polar atoms (estimated for hydrogen bonds) gives

$$\Delta C_p = 0.45\Delta A_{nonpolar} - 0.26\Delta A_{polar} \quad (4)$$

(Murphy & Freire, 1992). The predicted ΔC_p given by the above formula turns out to be -215 cal K^{-1} mol^{-1}, which is significantly less negative than the experimentally determined value of -468 ± 30 cal K^{-1} mol^{-1}.

Given the fact that ΔC_p is constant in the experimental range of temperatures, the enthalpy and the entropy changes can be expressed as linear functions of the heat-capacity change,

$$\Delta H^\circ = \Delta H^* + \Delta C_p(T - T_a^*), \quad (5)$$

$$\Delta S^\circ = \Delta S^* + \Delta C_p \ln(T/T_b^*), \quad (6)$$

where ΔH^* is the enthalpy change evaluated at an arbitrary temperature T_a^* and ΔS^* is the entropy change at a different temperature T_b^*. If the net change in enthalpy is considered to arise primarily from hydrophobic interactions and hydrogen bonds, $\Delta H = \Delta H_{hydrophobic} + \Delta H_{H\text{-}bond}$, then the hydrophobic component can be estimated from the model proposed by Baldwin (1986) based on the enthalpy of transfer of liquid hydrocarbons into water using an equation similar to (5), such that

$$\Delta H_{hydrophilic} = \Delta C_{p,nonpolar}(T - 295\ \text{K}),$$

where $\Delta H^* = 0$ and $T_a = 295$ K.

Thus, for the LdCyP–CsA complex $\Delta H_{hydrophobic}$ at 298 K turns out to be -0.8 kcal mol^{-1}. Since the measured ΔH at 298 K is -15.43 kcal mol^{-1}, it follows that the primary enthalpic stabilization at 298 K must arise from hydrogen bonds between LdCyP and CsA, five of which were identified in the complex crystal structure.

3.4.2. Binding free energy. The free energy of binding ΔG_{exp} remains at a fairly constant value of -10.60 kcal mol^{-1} at all temperatures (from 288 to 308 K) owing to 'enthalpy–entropy' compensation. The methodology proposed by Weng *et al.* (1997) has been used to analyze ΔG in terms of its energetic and entropic components. The free-energy change (ΔG) between two states (G_{bound} and G_{free}) can be postulated to be

$$\Delta G = (G_{bound} - G_{free}) = \Delta E + \Delta G_d - T\Delta S_c + \Delta G_{others}, \quad (7a)$$

where ΔE, ΔG_d and $T\Delta S_c$ represent the energy change, the desolvation free energy and the conformational entropy, respectively. ΔG_{others} includes all other free-energy contributions arising from vibrations, rotations, translations and protonation/deprotonation effects and was found to have a constant value of 11.2 kcal mol^{-1} for protein–protein complexes. The assumption of comparable packing densities around interfacial regions for interacting molecules in the free and bound forms leads to the cancellation of van der Waals energy terms and their negligible contribution to ΔE. Furthermore, given the ostensibly constrained main-chain geometry of the drug (which is a cyclic peptide) and the significantly low r.m.s.d. (0.40 Å for C$^\alpha$ atoms) between native and complexed cyclophilin, it is highly probable that in such a rigid-body interaction the conformational energy of either molecule remains unaltered upon binding. Thus, ΔE reduces to the electrostatic energy terms ($\Delta E_{el}^{r\text{-}h}$) and the change in conformational entropy arises from the interfacial side-chain atoms alone. With these considerations, (7*a*) is modified to

$$\Delta G = \Delta E_{\rm el}^{\rm r\text{-}l} + \Delta G_{\rm d} - T\Delta S_{\rm side\text{-}chains} + 11.2. \qquad (7b)$$

The electrostatic interaction energy $\Delta E_{\rm el}^{\rm r\text{-}l}$ from the crystal structure of the LdCyP–CsA complex as calculated using *CHARMM* led to a value of -7.10 kcal mol^{-1}. The desolvation free energies $\Delta G_{\rm d}$ and $\Delta\tilde{G}_{\rm d}$ were computed from the complex crystal structure (see §2) utilizing the ASP (atomic solvation parameter) model, where ~ in the expression signifies that only neutral side chains were considered in the calculation. $\Delta G_{\rm d}$ and $\Delta\tilde{G}_{\rm d}$ were found to be -20.4 and -19.8 kcal mol^{-1}, respectively. Weng and coworkers have proposed an empirical expression to estimate $\Delta\tilde{E}_{\rm el}^{\rm r\text{-}l}$ based on changes in solvent-accessible area for polar and nonpolar atoms upon complexation,

$$\Delta\tilde{E}_{\rm el}^{\rm r\text{-}l} = (16.6 \pm 1.4)\Delta A_{\rm nonpolar} - (14.4 \pm 2.5)\Delta A_{\rm polar}, \qquad (8)$$

which gave a value of -7.09 kcal mol^{-1} ($\Delta A_{\rm nonpolar} = -680.6$ Å^2, $\Delta A_{\rm polar} = -291.7$ Å^2). Thus, the good agreement between $\Delta G_{\rm d}$ (-20.4 kcal mol^{-1}) and $\Delta\tilde{G}_{\rm d}$ (-19.8 kcal mol^{-1}) on one hand and $\Delta E_{\rm el}^{\rm r\text{-}l}$ (-7.10 kcal mol^{-1}) and $\Delta\tilde{E}_{\rm el}^{\rm r\text{-}l}$ (-7.09 kcal mol^{-1}) on the other confirmed the relatively negligible contribution of protonation/deprotonation effects involving ionizable side chains to the free-energy change.

Freire and coworkers (Murphy & Freire, 1992; Xie & Freire, 1994) have given a free-energy expression based on the calorimetric observation of protein unfolding (at 298 K),

$$\Delta\tilde{G}_{\rm c}^{*} = 49.6\Delta A_{\rm nonpolar} - 19.1\Delta A_{\rm polar}, \qquad (9)$$

where the c in $\Delta\tilde{G}_{\rm c}^{*}$ indicates that the above relation is based on calorimetric measurements, * indicates the non-inclusion of conformational entropy and ~ indicates the removal of protonation/deprotonation effects by performing the experiment with a suitable choice of buffer. Thus,

$$\Delta\tilde{G} - \Delta\tilde{G}_{\rm c}^{*} = -T\Delta S_{\rm side\text{-}chain} + \Delta G_{\rm others}, \qquad (10)$$

where $\Delta\tilde{G}$ can be obtained from the experimentally determined binding free energy ΔG suitably corrected for the removal of protonation/deprotonation effects by adding $[(\tilde{E}_{\rm el}^{\rm r\text{-}l} - E_{\rm el}^{\rm r\text{-}l}) + (\Delta\tilde{G}_{\rm d} - \Delta G_{\rm d})]$. The side-chain entropy term $T\Delta S_{\rm side\text{-}chain}$ estimated by appropriate substitutions in (10) turns out to be $T\Delta S_{\rm side\text{-}chain} = -4.60$ kcal mol^{-1}, which is in good agreement with the experimentally derived value of -4.80 kcal mol^{-1}. The side-chain entropy $T\Delta S_{\rm side\text{-}chain}$ for LdCyP can be obtained using the empirical entropy scale of Pickett & Sternberg (1993), which gives a value of -3.55 kcal mol^{-1}. Thus, it follows that the entropic contribution of CsA should be in the region of -1 kcal mol^{-1}. Six residues of CsA (Mle9, Mle10, Mva11, Bmt1, Aba2 and Sar3) primarily interact with the receptor protein. A survey of 30 (NMR and X-ray) structures of cyclosporin A in cyclophilin–cyclosporin complexes indicated conformational variability in only two side chains (Bmt1 and Aba2), in contrast to Mle and Mva which consistently exhibited unique torsion angles (χ_1). Both Bmt ($\chi_1 = -50^\circ$ and -25°) and Aba ($\chi_1 = -60^\circ$ and -30°) exhibited two rotamers each. Estimation of entropy utilizing the classical definition $S_{\rm c} = -R\sum_i p_i \ln(p_i)$ assuming equally probable conformers (two for Bmt, two for Aba) leads to a value of -0.82 kcal mol^{-1} at 298 K. Inclusion of Mle (g^+, g^-, t) and Mva (g^+, g^-, t) in the calculation appears to systematically overestimate the entropic contribution of CsA to the binding free energy ΔG. Thus, on summing all the structure-based components contributing to the free-energy change, (7*b*) yields $\Delta G = -11.33$ kcal mol^{-1}, which is in reasonable agreement with the experimentally measured value of -10.60 kcal mol^{-1}.

4. Discussion

The fluorescence and ITC data confirm the tight binding ($K_{\rm d}$ in the nanomolar range) of CsA to its receptor LdCyP. However, there is a large divergence between the predicted (-215 cal K^{-1} mol^{-1}) and measured (-468 ± 30 cal K^{-1} mol^{-1}) values of $\Delta C_{\rm p}$. These differences between predicted and calorimetric values can occur when conformational changes in reactants accompany the binding process or if there are solvent molecules involved in the interactions at the binding interface (Morton & Ladbury, 1996). Furthermore, contributions from multiple protonation events can have significant effects on $\Delta C_{\rm p}$ which are not accounted for in the $\Delta C_{\rm p}$ computed from static structural information. It is notable that a similar calculation performed on CsA and human CyP gave a comparable value of -211 cal K^{-1} mol^{-1} (Fanghanel & Fischer, 2003), which also deviates substantially from the experimentally determined $\Delta C_{\rm p}$ of -435.8 ± 70 cal K^{-1} mol^{-1}. The involvement of solvent water molecules in the binding interface of human CyP–CsA has been proposed to explain this discrepancy. Five interfacial water molecules have been identified in the crystal structure of the human CyP–CsA complex solved at 2.1 Å resolution (Mikol *et al.*, 1993). Two of these five highly ordered water molecules make simultaneous hydrogen bonds to both the protein and drug, whereas the other three make hydrogen bonds *via* other water molecules. The thermodynamic effect of placing water molecules in the binding interface is currently not well understood. The contribution of such solvent waters to $\Delta C_{\rm p}$ seems to vary over a wide range from -17.0 to -106.0 cal mol^{-1} K^{-1} per water (Holdgate *et al.*, 1997). However, an average value of -48 ± 31 cal mol^{-1} K^{-1} per water has been used to account for the discrepancy in the human complex. Recently, another estimate assigned -57 ± 21 cal mol^{-1} K^{-1} per sequestered water at the CyP–CsA interface (Stegmann *et al.*, 2009). At the reported resolution, no water molecules were observed in the interface of the LdCyP–CsA complex. However, this does not rule out the identification of such solvent molecules at a more favourable resolution.

Given the good agreement between the measured change in free energy ($\Delta G_{\rm exp} = -10.60$ kcal mol^{-1}) and a predicted value based on structure-based calculations ($\Delta G = -11.30$ kcal mol^{-1}), it appears highly probable that the basic assumptions made during structure-based calculations are indeed valid. These would include (i) the enthalpic stabilization primarily being a consequence of intermolecular hydrogen bonds; (ii) 'rigid-body association' between drug and protein (also borne out by structural comparison between

native and complexed cyclophilin) such that the change in energy ΔE arising from conformational alteration during binding is negligible; (iii) cancellation of van der Waals energy terms owing to comparable atomic density surrounding interfacial residues before and after complexation; (iv) an entropy change that arises from side-chain conformations alone for both protein and drug and (v) a negligible contribution of protonation/deprotonation effects to the overall free-energy change.

Owing to the presence of unnatural amino acids and the availability of only a limited number of NMR and crystal structures of cyclosporin (in complex with cyclophilin), it is difficult to correctly assess the conformational space accessible to the interfacial side chains. It is highly probable (as per the calculation estimating ΔS for LdCyP) that the contribution of CsA to ΔS is of the order of -1.0 kcal mol^{-1}. Inclusion of all side chains found in the LdCyP–CsA interface appears to systematically overestimate ΔS owing to CsA. It could be possible that free CsA in an aqueous environment is already in a conformational state very similar to the bound form of the molecule. Although CsA has been shown to exhibit multiple conformations in nonpolar solvents, its conformation in the 'CyP-bound' form has been suggested to pre-exist in aqueous solutions (Altschuh *et al.*, 1992).

All atomic interactions between LdCyP and CsA are completely conserved in human and other trypanosomatid CyP–CsA complexes. It is certain that the relative insensitivity of *L. donovani* to the drug does not arise by virtue of the inability of parasitic cyclophilin to bind to the drug. Although Cn from *L. donovani* has not been characterized, its existence and similarity to the Cns from the genomes of other trypanosomatids is highly probable. In addition, phosphatase activity of a calcineurin-like protein has been detected in *L. donovani* (Banerjee *et al.*, 1999). Modelled CyP–CsA–Cn ternary complexes for *L. infantum*, *L. major*, *L. braziliensis* and *T. cruzi* (data not shown; based on a human template, PDB code 1m63) show conservation of the key residues that mediate the interaction between CsA and Cn in human by specific hydrogen bonds or hydrophobic contacts. However, significant variability is also observed in the parasitic CyP–Cn interface with respect to that in human. Owing to the variability in the CyP–Cn interface, a wide range of affinities between CyP–CsA and Cn can be expected, leading to differential sensitivity of the parasites to CsA.

The Centre for Applied Mathematics and Computational Science kindly provided computational facilities. Mr Sankar Basu is acknowledged for assistance in computer programming and Miss Grihanjali Devi, Mr Abhijit Bhattacharya and Mr Sekhar Bhattacharya for technical assistance. This work was supported by grants from the Council of Scientific and Industrial Research, India and from the intramural project MMDDA, Saha Institute of Nuclear Physics.

References

Aich, P., Sen, R. & Dasgupta, D. (1992). *Biochemistry*, **31**, 2988–2997.
Altschuh, D., Vix, O., Rees, B. & Thierry, J. C. (1992). *Science*, **256**, 92–94.
Baldwin, R. L. (1986). *Proc. Natl Acad. Sci. USA*, **83**, 8069–8072.
Banerjee, C., Sarkar, D. & Bhaduri, A. (1999). *Parasitology*, **118**, 567–573.
Brooks, B. R., Bruccoleri, R. E., Olafson, B. D., States, D. J., Swaminathan, S. & Karplus, M. (1983). *J. Comput. Chem.* **4**, 187–217.
Brünger, A. T. (1992). *Nature (London)*, **355**, 472–475.
Brünger, A. T., Adams, P. D., Clore, G. M., DeLano, W. L., Gros, P., Grosse-Kunstleve, R. W., Jiang, J.-S., Kuszewski, J., Nilges, M., Pannu, N. S., Read, R. J., Rice, L. M., Simonson, T. & Warren, G. L. (1998). *Acta Cryst.* D**54**, 905–921.
Bua, J., Fichera, L. E., Fuchs, A. G., Potenza, M., Dubin, M., Wenger, R. O., Moretti, G., Scabone, C. M. & Ruiz, A. M. (2008). *Parasitology*, **135**, 217–228.
Bua, J., Ruiz, A. M., Potenza, M. & Fichera, L. E. (2004). *Bioorg. Med. Chem. Lett.* **14**, 4633–4637.
Chakrabarti, S., Mir, M. A. & Dasgupta, D. (2001). *Biopolymers*, **62**, 131–140.
Cruz, M. C., Del Poeta, M., Wang, P., Wenger, R., Zenke, G., Quesniaux, V. F., Movva, N. R., Perfect, J. R., Cardenas, M. E. & Heitman, J. (2000). *Antimicrob. Agents Chemother.* **44**, 143–149.
DeLano, W. L. (2002). *The PyMOL Molecular Graphics System.* http://www.pymol.org.
Du, H., Guo, L., Fang, F., Chen, D., Sosunov, A. A., McKhann, G. M., Yan, Y., Wang, C., Zhang, H., Molkentin, J. D., Gunn-Moore, F. J., Vonsattel, J. P., Arancio, O., Chen, J. X. & Yan, S. D. (2008). *Nature Med.* **14**, 1097–1105.
Eisenberg, D. & McLachlan, A. D. (1986). *Nature (London)*, **319**, 199–203.
Fanghanel, J. & Fischer, G. (2003). *Biophys. Chem.* **100**, 351–366.
Fejzo, J., Etzkorn, F. A., Clubb, R. T., Shi, Y., Walsh, C. T. & Wagner, G. (1994). *Biochemistry*, **33**, 5711–5720.
Hertwig, R. H. & Koch, W. (1997). *Chem. Phys. Lett.* **268**, 345–351.
Holdgate, G. A., Tunnicliffe, A., Ward, W. H., Weston, S. A., Rosenbrock, G., Barth, P. T., Taylor, I. W., Pauptit, R. A. & Timms, D. (1997). *Biochemistry*, **36**, 9663–9673.
Jones, T. A., Zou, J.-Y., Cowan, S. W. & Kjeldgaard, M. (1991). *Acta Cryst.* A**47**, 110–119.
Kallen, J., Mikol, V., Taylor, P. & Walkinshaw, M. D. (1998). *J. Mol. Biol.* **283**, 435–449.
Ke, H. (1992). *J. Mol. Biol.* **228**, 539–550.
Keckesova, Z., Ylinen, L. M. & Towers, G. J. (2006). *J. Virol.* **80**, 4683–4690.
Laskowski, R. A., MacArthur, M. W., Moss, D. S. & Thornton, J. M. (1993). *J. Appl. Cryst.* **26**, 283–291.
Lee, B. & Richards, F. M. (1971). *J. Mol. Biol.* **55**, 379–400.
Mikol, V., Kallen, J., Pflugl, G. & Walkinshaw, M. D. (1993). *J. Mol. Biol.* **234**, 1119–1130.
Morton, C. J. & Ladbury, J. E. (1996). *Protein Sci.* **5**, 2115–2118.
Murphy, K. P. & Freire, E. (1992). *Adv. Protein Chem.* **43**, 313–361.
Page, A. P., Kumar, S. & Carlow, C. K. (1995). *Parasitol. Today*, **11**, 385–388.
Pickett, S. D. & Sternberg, M. J. (1993). *J. Mol. Biol.* **231**, 825–839.
Stegmann, C. M., Seeliger, D., Sheldrick, G. M., de Groot, B. L. & Wahl, M. C. (2009). *Angew. Chem. Int. Ed. Engl.* **48**, 5207–5210.
Sundar, S. & Murray, H. W. (2005). *Bull. World Health Organ.* **83**, 394–395.
Vajda, S., Weng, Z., Rosenfeld, R. & DeLisi, C. (1994). *Biochemistry*, **33**, 13977–13988.
Venugopal, V., Sen, B., Datta, A. K. & Banerjee, R. (2007). *Acta Cryst.* F**63**, 60–64.
Wang, P. & Heitman, J. (2005). *Genome Biol.* **6**, 226.
Wear, M. A. & Walkinshaw, M. D. (2006). *Anal. Biochem.* **359**, 285–287.
Weng, Z., Delisi, C. & Vajda, S. (1997). *Protein Sci.* **6**, 1976–1984.
Xie, D. & Freire, E. (1994). *Proteins*, **19**, 291–301.